Radiographics pattern recognition of welding defects using linear classifiers

R R da Silva, M H S Siqueira, L P Calôba and J M A Rebello

Radiographic inspection is widely used in non-destructive testing for integrity evaluation of structures and equipments, especially for detection and characterisation of defects in welded joints. For this reason, research to optimise this technique has been increasing in recent years. As it is a technique that demands the inspector's vast experience and correct adjustment of inspection parameters, in many situations the final decision becomes a difficult task and subject to interpretation mistakes. With the progress of computer science and techniques of artificial intelligence and neural computation, efforts in several countries have been made seeking the development of an automatic system of inspection for X-rays or gamma-rays that optimises the interpretation of welding defects. This work presents a way to obtain the best hierarchical and non-hierarchical linear discriminators for classification of the principal welding defects, using a neural network technique for implementation. The results prove the efficiency of the techniques used in the work.

Keywords: X-ray, pattern recognition, neural network, welding defects

1. Introduction

Nowadays, in times of globalisation and with the considerable increase in competition among industries, the quality control of equipment and materials becomes a fundamental tool in a company's survival. Non-destructive inspection techniques are a theme of research and development in industries and universities. Although it is one of the oldest techniques of non-destructive inspection, radiographic testing is still widely used in evaluating the structural integrity of equipment and materials. Several research centres in the world focus their objectives on the inspection optimisation for X-rays or gamma-rays.

Radiographic tests are also used in the evaluation of several processes of equipment production. However, their application is more common in the inspection of welded joints in industries such as nuclear, naval, chemistry, oil, aeronautics, etc.

The success of this technique is directly related to the appropriate control of the inspection parameters, which are regulated by standards. The correct interpretation of the X-ray image at the end of the test will depend essentially on the quality of the image and of the inspector's experience. Firstly, to identify the more common welding defects with X-rays, morphologic parameters are observed, such as geometric format, length, width, besides grey level (density) and location in the weld bead. As this evaluation is subjective, depending on the visual capacity of each inspector, it is necessary to improve this process by seeking a decrease in the interpretation error.

Parallel to the progress in computer science and the development of the sciences related to artificial intelligence, mainly in the fields of neural networks and fuzzy logic, research seeking the development of automatic systems of radiographic inspection has been increased considerably in recent years[1-8]. Most of these automatic systems involve a stage of digitalisation of the films (there are also equipments that generate digital images directly during the test[9]), a stage of the images preprocessing (application of digital filters and contrast improvement), and finally, a stage of defect detection. However, these stages are not strictly defined and they can, depending on the situation, involve other procedures, such as described by Liao[3-5].

The present work aims to obtain, through neural networks, the evaluation of the best hierarchical and non-hierarchical linear discriminators in welding defect classification: lack of penetration, undercutting, porosity, linear and non-linear slag inclusions.

2. Experimental methodology

2.1 Images acquisition

The radiographic films can be digitised by several systems according to ASME V[10]. The more common way of digitisation is through scanners, which works with light transmission - usually called transparency adapters. Another method also used is image acquisition by camera CCD (Charge Couple Device). In this case, the film is placed in the light box and the camera captures the digital image and transmits it for a computer. Aoki [1]comments the use of these two methods. Liao[3-5] and Jacobsen[6] have used scanners in their work on radiographic images acquisition. A detailed discussion about radiographic films digitisation may be found in the literature[11].

In order to improve the reliability in the results, radiographs from [1] IIW (International Institute of Welding) were used in a total of 86 films. These patterns have indications of the most frequent classes of defects in welded joints, such as lack of penetration, porosity, slag inclusion linear and non-linear, undercutting, etc. The X-radiographs were digitised in a flatbed scanner type UMAX Mirage II with a resolution of 400 dpi (dots per inch) and 256 grey levels, being stored in TIFF format (without compression).

2.2 Preprocessing of the images

After digitisation of the films, it is very common to use a preprocessing stage, seeking mainly the attenuation/elimination of noise and contrast improvement. The application of lowpass filters is the more frequently used tool to remove noise in a radiographic image[11,12]. The quality of radiographic images is related to the technique employed, as well as of the inspected material, as well as the choice of a standard filter for noise elimination. Therefore, the

Romeu R da Silva, Marcio H S Siqueira and João M A Rebello are in the Department of Metallurgical and Materials Engineering, Federal University of Rio de Janeiro (UFRJ), PO Box 68505, CEP 21945-970, Rio de Janeiro, RJ Brazil. E-mail: romeu@metalmat.ufrj.br

Luiz P Calôba is in the Department of Electrical Engineering, Federal University of Rio de Janeiro (UFRJ), PO Box 68504, CEP 21945-970, Rio de Janeiro, RJ Brazil. E-mail: caloba@lps.ufrj.br

[1] Properly authorised by International Institute of Welding.

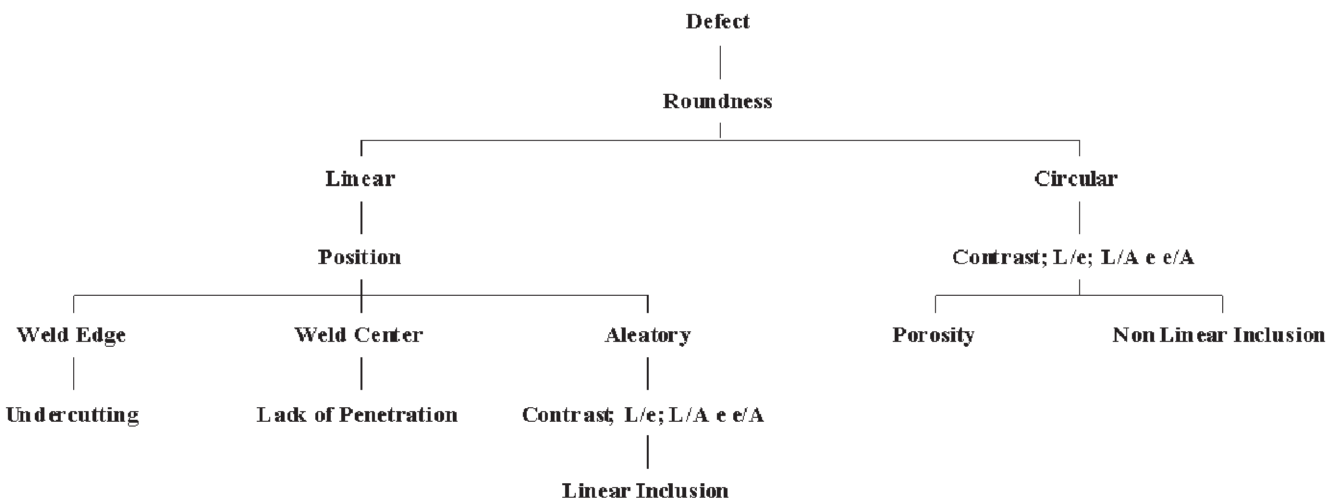

Figure 1. Chart representing the separation of the classes of defects through the used parameters

correct choice is usually made in an empirical way remembering that the employment of these filters must not change important information in the images. Some authors, such as Aoki[1], use other procedures such as background subtraction and segmentation for the region growing method to facilitate the identification of defects.

Two preprocessing stages were accomplished in this work: application of lowpass filter (median type) and contrast improvement for extension of the image's observed histogram. The execution of these stages was accomplished in the software Image Pro Plus 4.0 (Media Cybernetics).

2.3 Definition of the characteristic parameters of the defects

One of the most important stages in the development of an automatic system of radiographic inspection is the definition of the characteristic parameters of the defects. The appropriate choice of the most important characteristics in the identification of each class of defects has a fundamental importance in the recognition process by an intelligent system. This choice is made in way similar to the interpretation given by an inspector that, most of the time, recognises a type of welding defect in the radiograph image based on visual characteristics such as: location, shape, length, density (grey level), aspect ratio, etc., besides the observance of the welding conditions. Therefore, an important study of the morphology of the defect is demanded to optimise the performance of the system. Aoki[2] describes a system based on the use of 10 parameters for classification of five classes of defects. Kato[13] has worked with eight parameters for classification of seven types of defects. Liao[3-5] describes the use of three characteristic parameters in a classification algorithm that uses fuzzy logic. Lgraykia[14] has developed an automatic system based on image contrast and in the variation of grey levels for detection of defects, also using a system of fuzzy logic.

In the present work, six parameters are defined for discrimination of five classes of defects: non-linear slag inclusion (NLI), linear inclusion (LI), porosity (PO), lack of penetration (LP) and undercutting (UC). The amount of used data was composed by 15 undercutting observations, 14 of lack of penetration, 17 of porosity, 24 slag inclusions (non-linear) and 25 linear inclusions. Although, there are radiographic patterns regarding classes lack of fusion and cracks, these defects were not analysed because of absence of enough data for the classifiers generalisation. Figure 1 displays a flowchart with the rules used for choice of the parameters. Figure 2 displays a pattern example IIW, as well as the necessary dimensional measures for the calculation of each parameter.

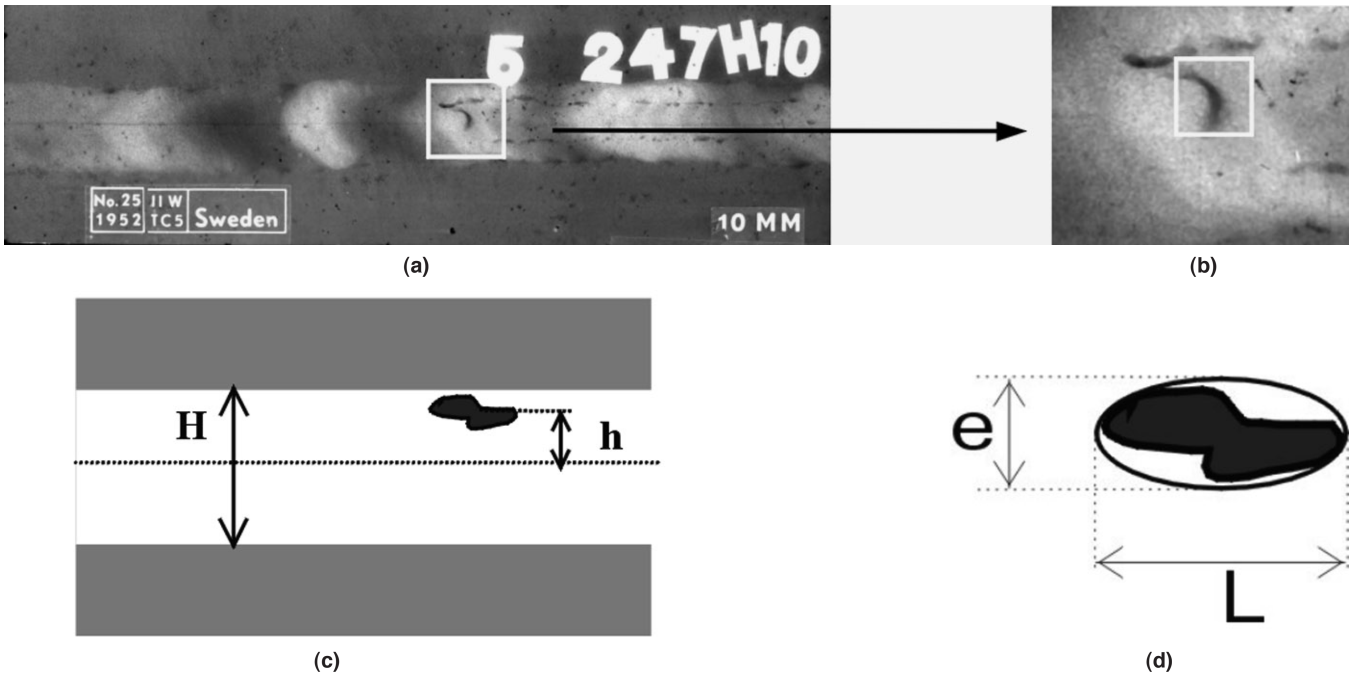

Figure 2. (a) Example of pattern IIW used; (b) presence of slag inclusion; (c) and (d) illustration for definition of the parameters used

Definition of the parameters used:

- *Contrast*: ratio between the variation of grey level in the defect (difference between the maximum and minimum value) and the grey level variation in the radiographic image. This parameter was chosen because each defect class possesses its degree of density. For instance: the defect 'lack of penetration' is usually darker than a slag inclusion.
- *Position* (p = h/H): this ratio supplies the location of the defect in relation to the centre of the weld bead. With this parameter it is possible to separate lack of penetration, frequently located in the bead centre, and undercutting, usually present at the border.
- *Aspect ratio* (a = L/e): this parameter is used for separation of the most spherical classes (porosity), values close to 1, and the less spherical ones (lack of penetration and linear inclusion). This parameter is calculated automatically in Image Pro (L is the largest axis of the smallest ellipse that includes the defect and **e** the smallest axis).
- *Ratio between width and area* (e/A): ratio between the smallest transverse length of the defect and its area. This information measures the circumference of the defect[1].
- *Ratio between length and area* (L/A): ratio between the largest horizontal length of the defect and its area. In this parameter L is the larger axis of the ellipse. This information measures the circumference of the defect[1].
- *Roundness*: ratio $p^2/4\pi A$, where p is the perimeter and A, area of the defect. By roundness, it is observed that when the shape of the defect approaches a circle, this measure will tend to 1. This is useful in the separation of the spherical defects such as porosity and non-linear slag inclusions and linear defects as lack of penetration, non-linear inclusions and undercutting.

In this work the vector $\vec{x}$ that characterises each defect pattern will be called 'input' of the system, and each parameter, or component of this vector, 'input component' or simply 'component'; each defect class will be denominated 'class'.

2.4 Data preprocessing

So that the extracted data are the most representative possible and do not hinder the construction of classifiers, it is important to eliminate atypical inputs (outliers) that are outside the true representation of a class. Based on this requirement, the measures of each one of the components of inputs were adjusted in a normal distribution and the atypical inputs, located more than three standard deviations away from the average, were excluded from the data group.

2.5 Non-hierarchical and hierarchical linear discriminators

Each input is represented by six parameters, that is, for a vector $\vec{x}$ of dimension 6, or geometrically, for a point in a space of dimension 6, called space of inputs.

A linear discriminator for class Cj separates the inputs of this class to the others through an equation of first order, linear:

$$\vec{x} \quad C_j \Leftrightarrow U_j > 0 \qquad (1)$$

where:

$$U_j = \sum_{i=1}^{6} w_{ji} x_j + b_j = \vec{w}^t_j + b_j \qquad (2)$$

Each class C_j has its own discriminator, defined for $\vec{w}_j$ and b_j.

In the input domain, the separator of the class C_j, that is, the locus of the points that satisfy $U_j=0$, is a perpendicular plan to the vector $\vec{w}_j$ and distant from the origin $-b_j / \left|\vec{w}_j\right|$, distance in the direction of $\vec{w}_j$. It is usually normalised $\left|\vec{w}_j\right| = 1$, being adjusted the value of b_j in a way so as not to change equation (1). In this case, U_j measures the distance of the input $\vec{x}$ to the separator, and it is a measure of the probability of success of the classification for that specific input.

A optimum discriminator is one of those that maximises the probability of success of the classification. The use of optimum linear discriminators is a well-known technique, denominated in statistics as *Fisher Discriminators*. A practical form of implementing them is through a neural network with a layer and, in this layer, a single neuron for class, as described by Haykin [15]. This technique was used in this work.

The geometric visualisation of the separators in this case is impossible due to the dimensions of the input space, but in a space of dimension 2, it can be easily accomplished. Consider Figure 3, where the shaded areas display the domain of inputs of hypothetical classes C_j and their respective plans separators S_j (that are represented by a straight line in this case).

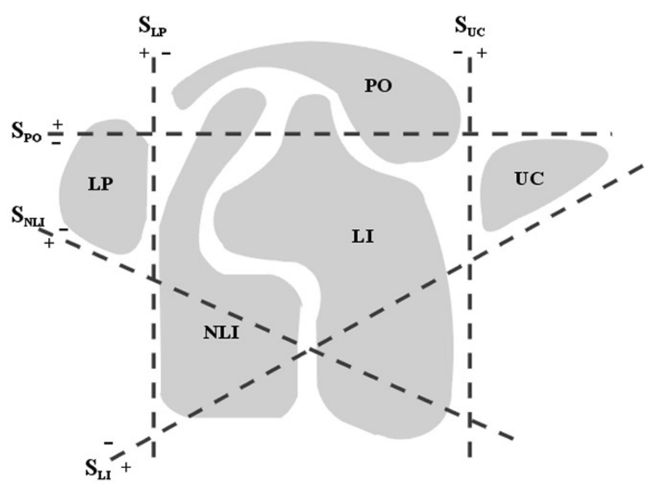

Figure 3. The five classes C_j, j = UC, LP, PO, LI, NLI, and their respective non-hierarchical separators S_j with suitable polarities. The most external classes UC and LP are perfectly separated and the most internal LI and NLI very imperfectly separated

Each separator S_j divides the input space into two semi-spaces (in this case two semi-plans), one where $U_j>0$ and another where $U_j<0$. Inputs that belong to the class C_j and that are correctly classified, are represented by points in the semiplane where U_j is positive. Notice that there are areas located in the positive semi-space of two or more separators: an input in this area will be allocated in two or more classes; on the other hand, there could be areas located in the negative semi-space of all the separators: an input in this area will not be allocated to any class. In this situation, we can use the fact that U_j is a measure of the probability of an input to belong to the class C_j and 'reclassification' the result, taking the class with largest U_j, the most probable of containing the input, as being the answer.

Let us also notice clearly that most 'external' classes are more easily separable, while the 'internal' ones are hardly separable, Figure 3. However, if these 'external classes' are removed, other classes previously 'internal' will become 'external', and now they can be easily separable, Figure 4. This procedure leads us to the concept of hierarchical classification, where initially the 'external classes' are classified, in other words, those with a high degree of success, and after, the 'interns'.

In the case of non-hierarchical discriminators, the $\vec{w}_j$ vector discriminator and the polarisation b_j for each one of the classes C_j in relation to the remaining ones were found. Both are normalised

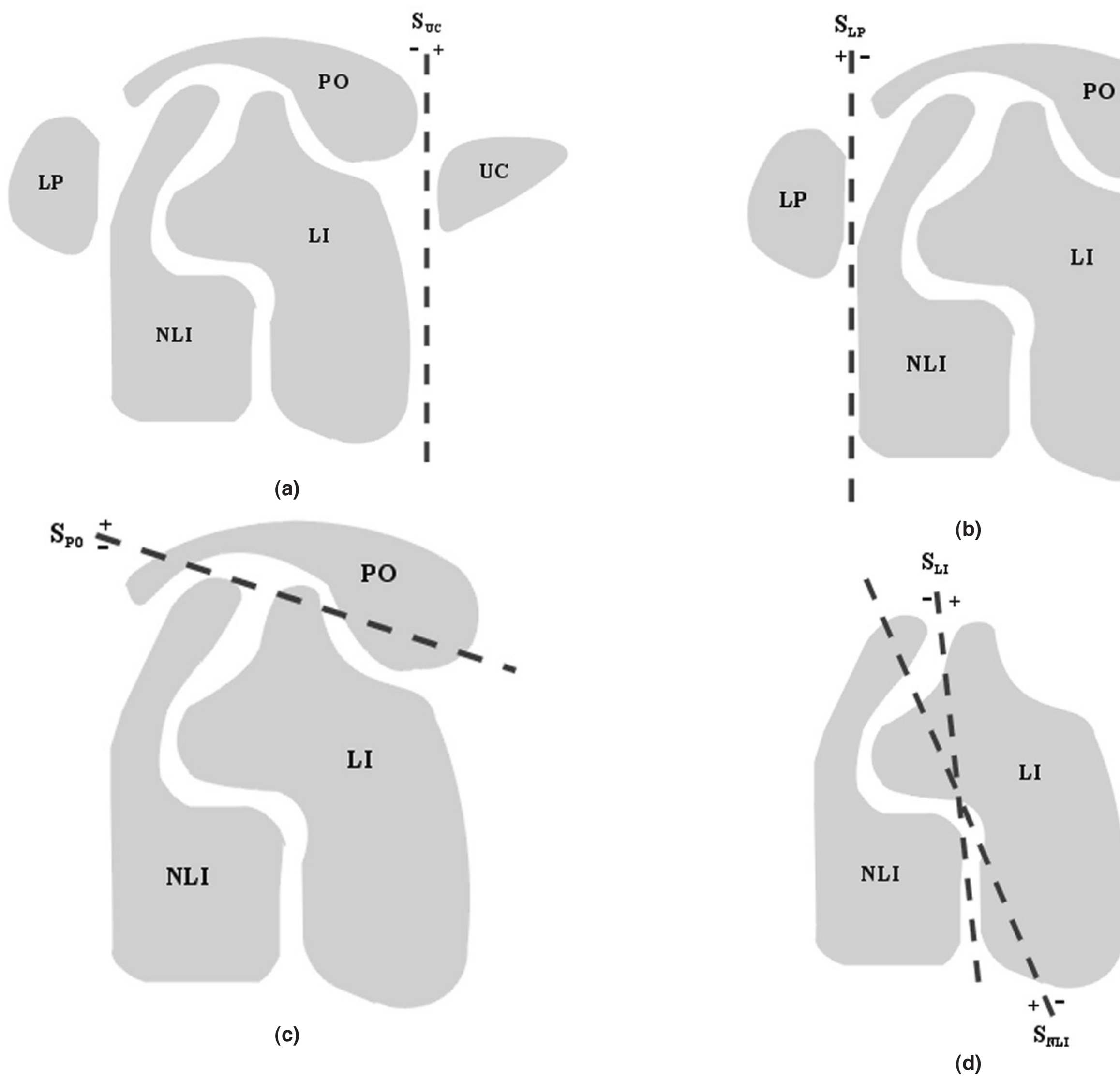

Figure 4. After the exclusion of the inputs classified as LP and UC, (a) and (b), the other discriminators can assume much more effective positions in the separation of the remaining classes, mainly S_{PO}, (c) and (d): the same happens after the exclusion of the inputs classified as PO

for a vector unitary module $\vec{w}_j$. In this case, the obtaining of the best possible discriminator is sought for a class to be separate from the remaining ones, not changing the input for the network training (Figure 3).

The hierarchical classifier is obtained in a similar way to the previous method, but for the training of each class Cj, the inputs that were already classified as belonging to more 'external' classes were picked up from the training date. The neuron corresponding to each class does not participate in the training of the following classes. Thus, the vectors $\vec{w}_j$ for the classes more easily separable are obtained in a hierarchical process. It is verified that the most 'internal' classes, and therefore, those which are more difficult to be separated in a non-hierarchical process, become more easily separable in this process, as shown in Figure 4.

2.6 Non-hierarchical and hierarchical classifiers

2.6.1 Non-hierarchical classifier

The flowchart of the non-hierarchical classifier is shown in Figure 5. The input vector $\vec{x}$ is multiplied by vector $\vec{w}_j$ of each class and added to the bias (b_j) generating U_j. The result of this operation is larger than zero and corresponds to the defect class. In this situation, there is the possibility of no class being indicated (when all the outputs are negative), or more than one indication (more than one output larger than zero). In this case, a reclassification criterion can be used, which the largest value of U_j indicates the class. For both cases, tables of defect confusion were built based on the obtained results, besides the successes, errors and non-classification table for this classifier structure.

2.6.2 Hierarchical classifier

Unlike the non-hierarchical classifier, the hierarchical classifier works by first classifying the more easily separable classes. The algorithm of this classifier is shown in Figure 6. The performance was verified in a similar way to the non-hierarchical classifier. The algorithms of the hierarchical and non-hierarchical classifier are compared in relation to success performance.

3. Results and discussions

3.1 Non-hierarchical classifiers

In this classifier, each class should be discriminated from all the others, independently of whether or not they are lineally separable. Table 1 displays the results found for a classifier without reclassification. In this case, the percentage values are also presented for when no class was identified or there were more than one activated class. According to Table 1, it is observed that in relation to the undercutting defect (UC), the success is 100%, indicating it to be separable by a linear discriminator. This result is due to the fact that this defect class has the parameter position very

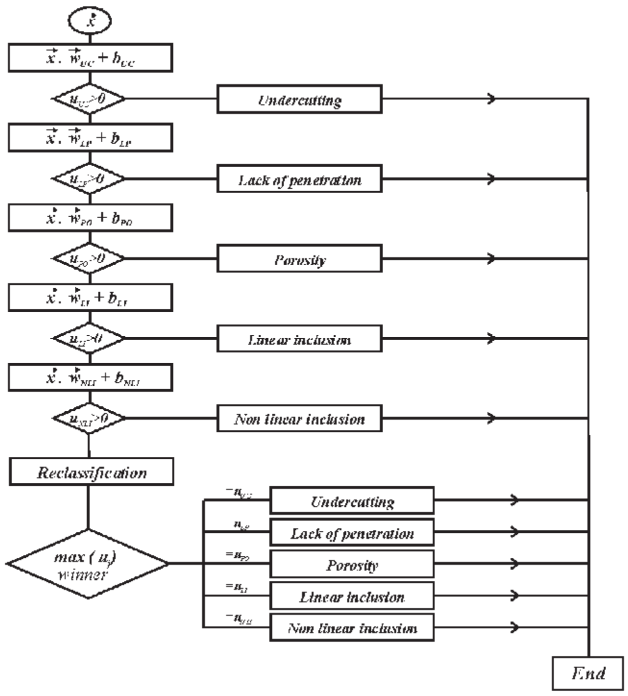

Figure 5. Algorithm of the non-hierarchical classifier

different from the others, located in the weld bead's edge or close to this. In relation to the defect lack of penetration (LP), the result shows that 14% of the observations resulted in a value up to zero, in more than one output of the classifier, indicating more than one class. For porosity (PO), the success is 77%, with 17% of multiple classification cases, also having 6% of percentage for the case of no indicated class. The results found for classes linear slag inclusion (LI) and non-linear (NLI) prove that the separation of these for a non-hierarchical linear process is complicated and the result was less satisfactory. This verification came from the fact that the classes PO, LI and NLI have different geometric formats and uncertain positions in the weld bead.

In Table 2 the performance percentage of the classifier are shown with reclassification based on the biggest output. In this case, it is easy to note that the classifier performance gets better, maintaining the success of 100% for MO and increased the PO for 100%, LP for 93%, LI for 64% and NLI for 63%, obtaining a good result for this classification type. As in radiographic testing the inspectors do not make the distinction between linear and non-linear inclusions, being both simply classified as slag inclusions;

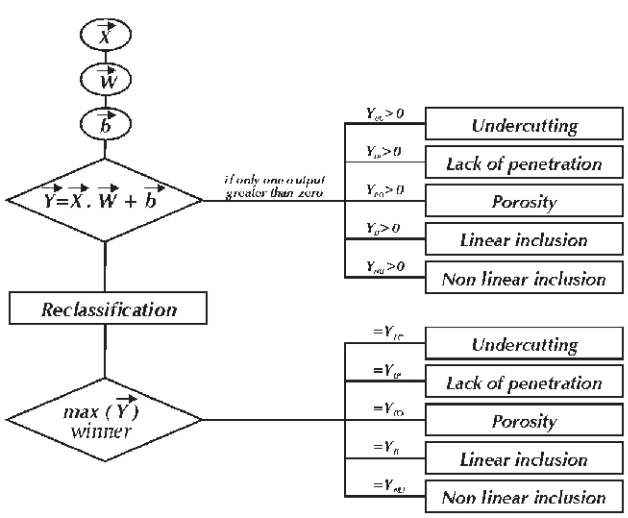

Figure 6. Algorithm of the hierarchical classifier

Table 1. Table of confusion (%)
Classifier non-hierarchical without criterion of reclassification

	UC	LP	PO	LI	NLI	More than one	None
UC	100					0	0
LP		86				14	0
PO			77			17	6
LI			4	36	8	0	52
NLI			4	8	42	4	42

Table 2. Table of confusion (%)
Classifier non-hierarchical with criterion of reclassification

	UC	LP	PO	LI	NLI
UC	100				
LP		93			7
PO			100		
LI	4		4	64	28
NLI		4	8	25	63

the percentage of success was verified for these classes together, resulting in a percentage reached of 90%.

Table 3 summarises the performance of these classifiers in relation to observations correctly classified, errors and outputs without classification (all negative outputs or more than one positive). First, for the case without criterion of reclassification in the output, and after with reclassification (Table 4). This way it was possible to define the general performance of this type of classification algorithm. The percentage found was 80% of success, - quite interesting after taking into consideration the architecture of employed classifier and the data amount used.

Table 3. Table of successes and errors
Classifier non-hierarchical without criterion of reclassification

	SUCCESSES	ERRORS	WITHOUT CLASSIFICATION
UC	15	0	0
LP	12	0	2
PO	13	0	4
LI	9	3	13
NLI	10	3	11
TOTAL	59 (62%)	6 (6%)	30 (32%)

Table 4. Table of successes and errors
Non-hierarchical with discriminators non-hierarchical with criterion of reclassification

	SUCCESSES	ERRORS
UC	15	0
LP	13	1
PO	17	0
LI	16	9
NLI	15	9
TOTAL	76 (80%)	19 (20%)

3.2 Hierarchical classifiers

Table 5 presents the results found for the hierarchical classifier. The performance of this classifier is better than the non-hierarchical classifier, even in the most rigorous criterion (classification when only one output is larger than zero). The indexes of 100% of success for UC and LP prove they are lineally discriminated from the others. For PO it was obtained 94% of success, existing confusion of 6% on observations with LI. For LI and NLI 72 and 75% of correct classifications was achieved, respectively. There is about 20% of confusion between these two classes, a value justified for the fact that they present very similar characteristic parameters. The results obtained with the criterion of reclassification in the output of the classifier, shown in Table 6, are the same ones as in the previous case, without increase of the percentage of success. On the other hand, the confusion between the class LI and PO increases from 4 to 8% and between NLI and LI increases from

Table 5. Table of confusion (%)
Hierarchical classifier without criterion of reclassification

	UC	LP	PO	LI	NLI	None
UC	100					0
LP		100				0
PO			94	6		0
LI			4	72	20	4
NLI			4	17	75	4

Table 6. Table of confusion (%)
Hierarchical classifier with criterion of reclassification

	UC	LP	PO	LI	NLI
UC	100				
LP		100			
PO			94	6	
LI			8	72	20
NLI			4	21	75

17 to 21%. This happened because in cases that occurred more than one positive output in the classifier, when using the criterion of reclassification, the indicated class was incorrect. However, it is not possible to conclude that this criterion does not supply better results because the number of observations was statistically insufficient.

Comparing the non-hierarchical with the hierarchical classifier, it is evident that results of this last one are better, mainly in relation to classes LI and NLI. In this case, considering the slag inclusion as just one class, the result is 96% of success to the Table 5 and 94% for Table 6. Tables 7 and 8 represent the general results of this classifier type. The index of 85% of success in Table 7 is considerably larger than the 62% of Table 3, also increasing from 80% of Table 4 to 85% of Table 8. This result can be considered quite good considering that a criterion of linear discriminator was used for defects classification and that Aoki[1] has obtained 92% of success for a system of non-linear discrimination with a neural network of two layers and 10 characteristic parameters of the defects slag inclusion (without separation between linear and non-linear), undercutting, porosity and lack of penetration. It is important to remember that in our study the classes of defect for cracks in welding and lack of fusion were not analysed because of absence of sufficient data for training and simulation of the classifiers; this will be considered by the authors in a future work.

4. Conclusions

Research on the development of automatic inspection systems for radiographic inspection has been increasing in recent years. The use of neural networks and systems using fuzzy logic are efficient, as expressed by the referred works [1-14, 16-18].

The results obtained in this work are really good for the proposed case. Only with non-hierarchical linear classifiers it was already possible to reach promising indexes of successes in the classification of some of the welding defects more frequently found in radiographic inspection. These indexes were still better when a classification algorithm based on a hierarchical criterion was used, in which the classes easiest to be separated are firstly treated for the classifier. The general percentage of 85% of success for this system is one of the best motivators for the continuation of work in this area. Hereafter, the defects such as lack of fusion and cracks will be analysed, as well as the use of non-linear discriminators for classification of defects.

Table 7. Table of successes and errors
Hierarchical classifier without criterion of reclassification

	SUCCESSES	ERRORS	WITHOUT CLASSIFICATION
UC	15	0	0
LP	14	0	0
PO	16	1	0
LI	18	6	1
NLI	18	5	1
TOTAL	81 (85%)	12 (13%)	2 (2%)

Table 8. Table of successes and errors
Hierarchical classifier with criterion of reclassification

	SUCCESSES	ERRORS
UC	15	0
LP	14	0
PO	16	1
LI	18	7
NLI	18	6
TOTAL	81 (85%)	14 (15%)

5. Acknowledgement

The authors wish to acknowledge CNPq, CAPES, FINEP and FUJB for financial support and scholarships and to International Institute of Welding for the permission given to publish the present work using the radiographic standards.

6. References

1. Aoki K, Suga Y, 'Intelligent Image Processing for Abstraction and Discrimination of Defect Image in Radiographic Film', Proceeding of the Seventh International Offshore and Polar Engineering Conference, Honolulu, USA, May 25-30, pp 527-531, 1997.
2. Aoki K, Suga Y, 'Application of Artificial Neural Network to Discrimination of Defect Type Automatic Radiographic Testing of Welds', ISI International, Vol 39, No 10, pp 1081-1087, 1999.
3. Liao T W, Ni J, 'An Automated Radiographic NDT System for Weld Inspection: Part I – Weld Extraction', NDT&E International, Vol 29, No 3, pp 157-162, 1996.
4. Liao T W, Ni J, 'An Automated Radiographic NDT System for Weld Inspection: Part II – Flaw Detection', NDT&E International, Vol 31, No 3, pp 183-192, 1998.
5. Liao T W, Li D and Li Y, 'Extraction of Welds from Radiographic Images using Fuzzy Classifiers, Information Sciences', Vol 126, pp 21-40, 2000.
6. Jacobsen C, Zscherpel U and Nockemann C, 'Crack Detection in Digitized Radiographs with Neuronal Methods', 7th European Conference on Non-Destructive Testing, Copenhagen, pp 2717-2724, 26-29 May, 1998.
7. Jagannathan H, Bahaskar N *et al*, 'A Step Towards Automatic Defect Pattern Analysis and Evaluation in Industrial Radiography using Digital Image Processing', 15th World Conference on Non-Destructive Testing, Rome, 15-21 October, 2000.
8. Nafaâ N, Redounane *et al*, 'Weld Defect Extraction and Classification in Radiographic Testing Based Artificial Neural Networks', 15th World Conference on Non-Destructive Testing, Rome, 15-21 October, 2000.
9. Gueudre C, Moysan J and Corneloup G, 'Geometric Characterization of a Circumferential Seam by Automatic Segmentation of Digitized Radioscopic Images', NDT&E International, Vol 30, No 5, pp 279-285, 1997.
10. ASME 5. Article II, Mandatory Appendix III. Digital Image Acquisition, Display and Storage for Radiography and Radioscopy, pp 36-37, 1995.
11. Da Silva R R, 'Images Processing Radiographic and Analysis of Defects in Weld Bead', Master's Degree, PEMM/COPPE/UFRJ, April, 1999.
12. Murakami K, 'Image Processing for Nondestructive Testing, Welding International', Vol 4, No 2, pp 144-149, 1998.
13. Kato Y, Okumura T and Matsui S *et al*, 'Development of an Automatic Weld Defect Identification System for Radiographic

Testing', Welding in the Word, Vol 30, No 7/8, pp 182-188, 1992.
14. Lashkia V, 'Defect detection in X-ray images using fuzzy reasoning', Image and Vision Computing 19, pp 261-269, 2001.
15. Haykin S, Neural Networks – A Comprehensive Foundation, Macmillian College Publishing. Inc., 1994.
16. Sankaran V, Chartrand B and Millard D *et al*, 'Automated Inspection of Solder Joints-A neural Network Approach', European Journal Mechanical Engineering, Vol 43, No 3, pp 129-153.
17. Zhang Z, Basart, P, 'Feature Extraction and Classification in Automated Inspection of NDE Images', Review of Progress in Quantitative Nondestructive Evaluation, Vol 14, pp 741-746, 1995.
18. Keck R, Coen G, 'Automatic Analysis of Defect Images in Radiographic Inspection, Metallurgical Plant and Technology', Vol 4, pp 66-67, 1998.